Early Detection of Parkinson's Disease by Neural Network Models

CHIN-HSIEN LIN[ID][1], FU-CHENG WANG[ID][2], (Senior Member, IEEE), TIEN-YUN KUO[2], PO-WEI HUANG[2], SZU-FU CHEN[3,4], AND LI-CHEN FU[ID][5], (Fellow, IEEE)

[1]Department of Neurology, National Taiwan University Hospital, Taipei 100, Taiwan
[2]Department of Mechanical Engineering, National Taiwan University, Taipei 106, Taiwan
[3]Department of Physical Medicine and Rehabilitation, Cheng Hsin General Hospital, Taipei 112, Taiwan
[4]Department of Physiology and Biophysics, National Defense Medical Center, Taipei 114, Taiwan
[5]Department of Computer Science & Information Engineering, National Taiwan University, Taipei 106, Taiwan

Corresponding author: Fu-Cheng Wang (fcw@ntu.edu.tw)

ABSTRACT This paper develops neural network models that can recognize Parkinson's disease (PD) at its early stage. PD is a common neurodegenerative disorder that presents with progressive slow movement, tremor, limb rigidity, and gait alterations, including stooped posture, shuffling steps, festination, freezing of gait, and falling. Early detection of PD enables timely initiation of therapeutic management that decreases morbidity. However, correct recognition of PD, especially in early-stage disease, is challenging because the aging population, which has a high PD prevalence, also commonly exhibits progressive gait slowness due to other disorders, such as joint osteoarthritis or sarcopenia. Therefore, developing a reliable and objective method is crucial for differentiating PD gait characteristics from those of the normal elderly. The aim of this study was to develop neural network models that could use the participants' motion data during walking to identify PD. We recruited 32 drug-naïve PD patients with variable disease severity and 16 age/sex-matched healthy controls, and we measured their motions using inertial measurement unit (IMU) sensors. The IMU data were used to develop neural network models that could identify patients with advanced-stage PD with an average accuracy of 92.72% in validation processes. The models also differentiated patients with early-stage PD from normal elderly subjects with an accuracy of 99.67%. Another independent group of participants recruited to test the developed models confirmed the successful discrimination of PD-affected from healthy elderly, as well as patients at different severity stages. Our results provide support for early diagnosis and disease severity monitoring in patients with PD.

INDEX TERMS Parkinson's disease, PD stage, IMU, neural network, gait.

I. INTRODUCTION

The aging of today's society is associated with an increasing number of patients suffering from neurodegenerative disorders. One of these disorders is Parkinson's disease (PD), and current estimates indicate that the number of people with PD will rise more than twofold, from 4 million in 2005 to 9 million by 2030 [1]. The clinical presentations of PD include progressively slowing movements, limb rigidity, rest

tremor, and posture instability [2]. Unfortunately, even those patients who receive dopaminergic treatment or deep brain stimulation still deteriorate with increasing age, and their mortality rate is two- to three-fold higher than that of the general population [3]. Therefore, recognizing PD in its early stage is critical for initiating proper treatments to decrease morbidity and ease the medical burden in the elderly.

The clinical severity of PD can be divided into five stages, called the Hoehn-Yahr Stages I–V [4]. In Stage I, the patients experience unilateral symptoms, such as asymmetrical gait or hand swing; in Stage II, the disease influences are bilateral

The associate editor coordinating the review of this manuscript and approving it for publication was Laura Celentano.

and the patient's stability degrades; in Stage III, the disease affects the central reflex mechanism, and the patient tends to fall because of trunk instability; in Stage IV, the patient needs a wheelchair and other assistive devices; and in Stage V, the patient is wheelchair bound or even bedridden. Patients with PD can be classified as having early-stage or advanced-stage disease. In its early stages, denoted in this paper as Early_PD and defined as Hoehn-Yahr Stage ≤2, the symptoms include asymmetrical movement reduction of one limb, asymmetrical hand movements, and shuffling when walking, with a preserved posture reflex [5]–[7]. In the advanced stages, denoted here as Adv_PD and defined as Hoehn-Yahr Stage >2, the symptoms are more progressed and include postural reflex losses, festinating gaits that cause walking instability, and increased risk of falling.

However, early detection of PD is challenging because the normal aging population might also exhibit progressive gait slowness, termed senile gait, due to joint osteoarthritis or sarcopenia [8], [9]. Therefore, the aim of the present study was to develop a neural network model that could help physicians recognize the PD gait based on motion characteristics occurring during walking. The model would also facilitate monitoring of the PD disease severity stages for appropriate medication adjustment and intervention.

Advances in technology are now improving the early, timely, and accurate diagnosis of PD, especially when machine-learning techniques are applied. For example, Saad *et al.* [10] designed a Bayesian classifier that used features derived from video images to recognize freezing of the gait in patients with PD. Similarly, Tripoliti *et al.* [11] extracted features from multiple inertial measurement units (IMUs) and detected the freezing of gait with an accuracy of 96.11% by applying a Random Forest algorithm. Rocha et al. [12] analyzed gait parameters associated with skeleton joints provided by the Kinect and was able to distinguish three groups: Non-PD subjects, PD patients in the STIM ON state, and PD patients in the STIM OFF state. Daliri [13] proposed a diagnosis method to differentiate subjects with PD from healthy control subjects using the ground reaction forces obtained from sensors underneath both feet.

Wahid *et al.* [14] applied a multiple regression normalization strategy to extract gait characteristics and applied three machine-learning strategies to recognize PD. In that study, the Random Forest algorithm achieved the highest accuracy of 92.6%. Caliskan et al. [15] applied a deep neural network (DNN) classifier to diagnose PD based on a public speech data set. Compared with other traditional methods, the DNN model provided a better accuracy of 86.10%. Baby *et al.* [16] applied wavelet transformations to obtain gait features from vertical ground reaction forces, and they developed an artificial neural network that classified patients with PD with an average accuracy of 86.75%. Samà *et al.* [17] used data collected from a triaxial accelerometer placed on the waists. Application of support vector machines (SVMs) detected bradykinesia in patients with PD with an accuracy of 90%.

Kim *et al.* [18] proposed a tremor assessment system that quantified PD severity with an accuracy of 0.85 using a convolutional neural network and the accelerometer and gyroscope signals from a wrist module. Haq *et al.* [19] compared the performance of DNN with other machine-learning methods using public voice signals. The DNN outperformed other approaches and showed an accuracy of 98%, a specificity of 95%, and a sensitivity of 99%. Bilgin and Akin [20] used public force data and proposed multilayer perceptron neural networks to distinguish amyotrophic lateral sclerosis (ALS) from other neurodegenerative diseases, such as PD and Huntington disease (HD). They applied leave-one-out cross validation, which gave an accuracy of 82.14%, 78.79, and 96.55% in discriminating ALS from PD, HD, and healthy controls, respectively.

Abdulhay *et al.* [21] extracted features from public gait data and applied machine-learning techniques to achieve an accuracy of 92.7% for diagnosing PD. Rastegari *et al.* [22] calculated gait features based on signals from shoe sensors and developed a feature selection method to recognize three groups: healthy elderly persons, geriatric persons, and patients with PD. Hoang *et al.* [23] applied vertical ground forces from a public data set to develop a stacked convolutional neural network that could classify gaits between patients with PD and healthy controls with an accuracy of 88.7%. Hu *et al.* [24] proposed a graph convolution neural network to detect freezing of gait by visual information and achieved an accuracy of 0.887 in the experiments. Solana-Lavalle *et al.* [25] applied k-nearest neighbor (KNN), multilayer perceptron, SVM, and Random Forest to detect patients with PD using public vocal features. The models could detect PD with an accuracy of 94.7%, a sensitivity of 98.4%, a specificity of 92.68%, and a precision of 97.22%.

Sivaranjini and Sujatha [26] applied the AlexNet model to detect PD based on normalized public magnetic resonance imaging data. The results showed an accuracy of 88.90%, a sensitivity of 89.30%, and a specificity of 88.40% in recognizing PD. Aydin and Aslan [27] applied the ViBe algorithm and the Hilbert-Huang transform and were able to recognize patients with PD with an accuracy of 98.79% using the gait features derived from sensors on the bottom of feet. Maachi *et al.* [28] proposed a DNN, which used gait features extracted from ground reaction forces, to identify PD severity with an accuracy of 85.3%. Karan and Sahu [29] combined variational mode decomposition and Hilbert spectrum analysis to select features from speech signals for investigation of voice tremor in patients with PD. The model could classify PD with an accuracy of 91% and 96% with the vowel /a/ and the word /apto/, respectively. Gunduz [30] proposed a PD diagnosis system that applied vocal features and classified PD with an accuracy of 91.6%.

Similar techniques have been applied for the recognition of patients with mild cognitive impairment (MCI). For example, Yang *et al.* [31] applied functional near-infrared spectroscopy (fNIRS) signals to recognize patients with MCI and achieved an accuracy of 60%, 76.67%, and up

to 90.62% using a statistical method, linear discriminant analysis (LDA), and a convolutional neural network (CNN), respectively. Yang *et al.* [32] then extracted three types of features from the fNIRS signals and identified MCI patients with an accuracy of 90.37% by applying CNN models. Yoo *et al.* [33] proposed a channel-wise feature extraction method for the fNIRS data to diagnose MCI patients. They then applied LDA and SVM to achieve an accuracy of 83.33%. Yang *et al.* [34] applied the VGG19 pre-trained CNN model and the classification-based transfer learning method to the temporal features from fNIRS signals at the resting state. Their model could recognize MCI patients with an accuracy of 97.01%.

Because the feature extraction process could have altered important signal characteristics, Guayacán and Martínez [35] proposed a 3D convolutional network to recognize patients with PD from gait videos without extracting special features. Their model classified PD with an accuracy of 94.89 by highlighting the spatiotemporal patterns. In the present study, we measured the participants' motion data and directly applied those data to develop a neural network model capable of distinguishing a PD gait from that of a healthy elderly person, while also differentiating Early_PD from Adv_PD with high accuracy as a surrogate disease-monitoring gait marker for disease progression. This paper is arranged as follows: Section II describes the experimental settings. We recruited PD patients and age- and gender-matched healthy participants for the experiments and measured their motions by IMUs. Section III introduces the structure of the neural network models for detecting PD and its stages. Because the symptoms of PD might vary as the stage progresses, the model consists of two sub-models that classify the data as Adv_PD, Early_PD, or Non-PD. Section IV presents the model development procedures, in which we applied the k-fold cross-validation method for model training and validation. New subjects were then recruited to test the developed models. Finally, we draw conclusions in Section V.

II. DATA COLLECTION

This section describes the experiments conducted to collect the clinical data. We invited patients with PD and healthy elderly control subjects to participate in the tests. Their kinematic data were measured by IMUs and applied to develop the neural network model for detecting PD and classifying its stages.

We recruited 32 patients with PD and measured their clinical motion data. The recruitment criteria for selecting patients with PD included: (1) a diagnosis of PD based on the United Kingdom PD Society Brain Bank clinical diagnostic criteria [36]. (Patients were excluded if they had signs of atypical parkinsonism or other secondary cause–related parkinsonism features); (2) a Hoehn-Yahr Stage [4] determined by an experienced movement disorder specialist (Dr. Lin CH); (3) the absence of any other musculoskeletal disorders that might influence the typical PD motions; (4) the ability to walk ten meters indoors without support

TABLE 1. Basic data of the participated subjects.

	Subjects with PD				Health Control Group		
No.	Gender	Age	Stage	Side	No.	Gender	Age
PD1	M	72	I	R	N1	F	67
PD2	F	64	I	L	N2	F	62
PD3	F	67	I	L	N3	F	69
PD4	M	52	I	R	N4	M	56
PD5	F	69	I	R	N5	M	77
PD6	F	67	I	L	N6	F	58
PD7	M	68	I	R	N7	M	76
PD8	F	73	II	L	N8	M	61
PD9	F	81	II	L	N9	F	57
PD10	F	65	II	L	N10	M	76
PD11	M	69	II	L	N11	F	78
PD12	F	53	II	R	N12	F	64
PD13	M	62	II	L	N13	F	60
PD14	M	49	II	L	N14	F	66
PD15	M	74	II	L	N15	M	85
PD16	M	66	II	L	N16	F	63
PD17	M	79	III	R			
PD18	F	56	III	L			
PD19	M	77	III	R			
PD20	M	84	III	R			
PD21	F	74	III	L			
PD22	M	70	III	R			
PD23	M	73	III	R			
PD24	F	61	III	R			
PD25	M	78	III	R			
PD26	M	79	III	L			
PD27	F	72	III	R			
PD28	F	66	III	L			
PD29	M	72	III	R			
PD30	F	70	IV	L			
PD31	M	75	IV	L			
PD32	F	80	IV	L			

or aid devices; and (5) a Mini-Mental State Examination [37] score higher than 24. We also recruited sixteen age- and sex-matched healthy subjects as the control group. All subjects' data are listed in Table 1; the designations PD1–PD16 indicate the patients with Early_PD, while PD17–PD32 indicate patients with Adv_PD, and N1–N16 are the healthy elderly controls. The patients' stages and affected sides were evaluated by doctors who had more than 15 years of daily experience with PD patients. All test subjects signed informed consent forms approved by the Institutional Review Board of National Taiwan University Hospital (IRB number: 202012017RINA), as shown in Appendix A, before joining the study.

We applied the APDM OPAL system [38] with wearable IMUs to record each subject's kinematic data. Wearable IMUs have frequently been used in motion analyses [11], [15], [17], [19] because of their advantages of portability, low cost, and fast data acquisition. In this paper, we developed a neural network model based on the data measured by the OPAL system. The specifications of the IMU system are illustrated in Table 2. Because PD might influence a patient's motions as the disease progresses, we attached five IMUs to each subject's shanks, lower arms, and waist, as shown in Figure 1.

During the experiments, all subjects were required to walk at their most comfortable pace, forward and back, along

TABLE 2. Specifications of the OPAL IMU system [25].

Dimensions	43.7 x 39.7 x 13.7 mm
Weight	< 25 g (with battery)
Resolutions	17.5 bits
Sampling rates	20 to 128 Hz
Transmission range	30m line of sight
Ranges of the accelerometer	± 200g
Ranges of the gyroscope	± 2000 deg/s
Ranges of the magnetometer	± 8 Gauss

(a) on the shanks

(b) on the lower arms

(c) on the waist
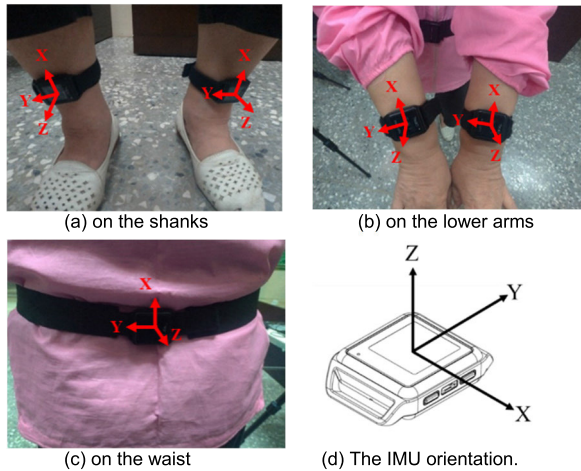
(d) The IMU orientation.

FIGURE 1. The IMUs for experiments.

a straight line about ten meters in length. A research assistant accompanied each subject because of safety concerns about the patients with PD. Each IMU recorded the 3-axial accelerations and 3-axial angular velocities with a sampling rate of 128 Hz. These measured data revealed that patients with PD at different stages tended to have varied IMU responses. For example, Figure 2 shows the angular velocities of the left shanks of subjects N16, PD7, and PD29 on the sagittal plane [39] (i.e., ω_y in Figure 1(a)). Notably, each gait cycle contains three important gait events [40]: mid-swing (MS), heel-strike (HS), and toe-off (TO).
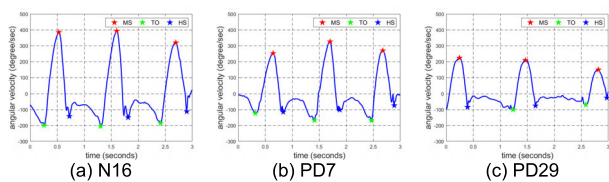

(a) N16

(b) PD7

(c) PD29

FIGURE 2. Angular velocities of the left shank on the sagittal plane.

A complete gait cycle comprised a stance phase (from HS to TO) and a swing phase (from TO to HS), which took about 60% and 40%, respectively, of the gait cycle duration in healthy persons. The MS usually happened when the angular velocity reached its maximum in the gait cycle; therefore, we were able to further divide the gait responses into gait cycles according to the MS events, as shown in Figure 3. Note that the gait cycles tended to be smoother and more regular in

the healthy subjects than in the patients with PD, whose gaits contained trembles and vibrations. However, distinguishing patients with PD from the healthy elders was still challenging, as the elderly healthy subjects also tended to have similar gait slowness and quakes because of other disorders. In addition, the swing phases tended to be shorter in the Adv_PD subjects than in the Early_PD subjects or the control groups. For instance, subject PD29 had a noticeably longer stance phase and a shorter swing phase because of a festinating gait, which caused a shorter swing phase but a faster speed and easily led to falling forward.
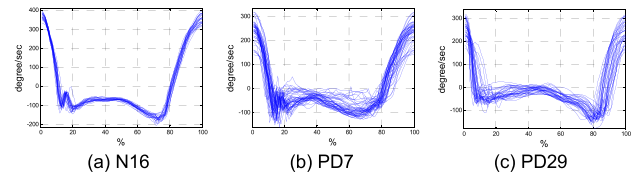

(a) N16

(b) PD7

(c) PD29

FIGURE 3. Left gait cycles.

Apart from the differences in gait responses, the arm swing was also an important differentiating characteristic of patients with PD, especially at the different stages. For example, the angular velocities of the lower arms on the sagittal plane (i.e., ω_z in Figure 1(b)) for subjects N16, PD7, and PD29 are illustrated in Figure 4. Because PD usually affects one side unilaterally at the early stage, subject PD7 tended to have a more asymmetrical arm swing when compared with subjects N16 and PD29. This difference could be a significant feature for distinguishing Early_PD.
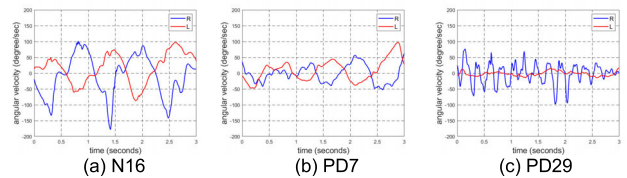

(a) N16

(b) PD7

(c) PD29

FIGURE 4. Swing of the lower arms on the sagittal plane.

These limb responses are normally applied to identify PD and to classify its stages. However, this evaluation is often subjective, meaning that different clinicians might arrive at different diagnoses. Therefore, we need an objective method for detecting PD and classifying its stages. In the next section, we apply the IMU data to develop a neural network model that can differentiate Adv_PD, Early_PD, and healthy elderly groups.

III. NEURAL NETWORK MODELS FOR PD RECOGNITION
This section applies the clinical IMU data to develop a neural network model for detecting PD and its stages. Many machine-learning methods are available, including KNN, SVM, and Random Forest [41]. Among them, neural networks have the advantages of exploring large amounts of input data and automatically selecting the operation to extract
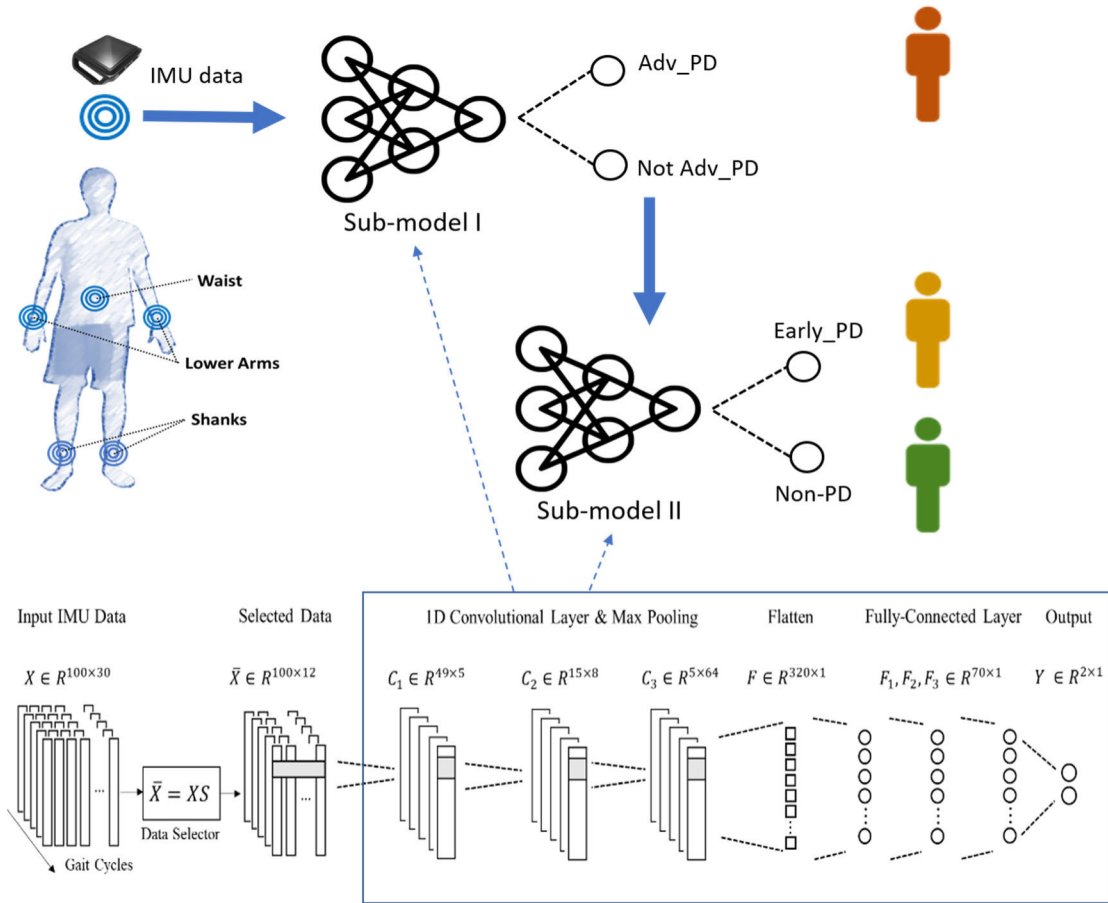
C.-H. Lin *et al.*: Early Detection of Parkinson's Disease by Neural Network Models

IEEE *Access*

FIGURE 5. Architecture of the neural network models.

data features that can support nonlinear transformations with high accuracy and robustness [42], [43]. Therefore, we proposed a neural network model to identify PD and classify its stages. The model comprised two sub-models: sub-model I and sub-model II. Sub-model I estimates whether the input IMU data are Adv_PD, while sub-model II classifies the input data as Early_PD or Non-PD if the IMU data are not Adv_PD. The architecture of the models is shown in Figure 5 and consists of the input layer, three convolutional layers, the flatten layer, three fully connected layers, and the output layer.

We integrated the synchronized IMU data as the model input. We first separated the IMU data according to the MS events of the gait responses because the gait motions were repeated and periodic. The IMU data were partitioned according to the MS events on the left or right sides, depending on which side was affected. We then normalized the IMU data by dividing them into one hundred points in each gait cycle, because the subjects might have varied their walking speeds and the data length may have differed in each gait cycle. Finally, we constituted the input data, as follows:

$$X = \begin{bmatrix} X_{RF} & X_{LF} & X_{RA} & X_{LA} & X_W \end{bmatrix}, \quad (1)$$

where the subscripts RF, LF, RA, LA, and W represent the IMU data measured from the right foot, left foot, right arm, left arm, and waist, respectively. Each IMU data point also consisted of 3-axial angular velocities and 3-axial accelerations, as follows:

$$\begin{aligned} X_i &= \begin{bmatrix} \omega_i & a_i \end{bmatrix} \\ &= \begin{bmatrix} \omega_i^x & \omega_i^y & \omega_i^z & a_i^x & a_i^y & a_i^z \end{bmatrix}, \quad (2) \end{aligned}$$

in which $\omega_i \in R^{100\times3}$ and $a_i \in R^{100\times3}$, for $i = RF$, LF, RA, LA, or W. That is, the input X is a combination of five IMUs with a dimension of 100×30. The subjects' IMU data are provided in Appendix B. As an example, an input X from PD22 is shown in Appendix C, where the IMU data were synchronized and partitioned by the left MS. Because the characteristics of the IMU data cannot be easily connected to the motions associated with PD, we developed a neural network to identify PD and its severity.

We then applied a selection matrix to pick suitable data for the two sub-models. For sub-model I, we chose the IMU data on the affected side by setting the selection

VOLUME 10, 2022

19037

matrix S_1 as follows:

$$S_1^R = \begin{bmatrix} I_{6\times6} & 0 \\ 0 & 0 \\ 0 & I_{6\times6} \\ 0 & 0 \\ 0 & 0 \end{bmatrix}_{30\times12},$$

$$S_1^L = \begin{bmatrix} 0 & 0 \\ I_{6\times6} & 0 \\ 0 & 0 \\ 0 & I_{6\times6} \\ 0 & 0 \end{bmatrix} \in R^{30\times12}. \quad (3)$$

The reason for doing this was that Adv_PD tends to have freezing arm movements and gait disorders (e.g., tremors and short swing phases) that affect the foot motions, especially on the affected side. For example, we set $\bar{X} = XS_1^R = [X_{RF} \ X_{RA}]$ for PD1 because the affected side was the right side, while we set $\bar{X} = XS_1^L = [X_{LF} \ X_{LA}]$ for PD2 because the affected side was the left side.

Similarly, we chose the angular velocities on both arms and the waist IMU data for sub-model II by setting the selection matrix S_2 as follows:

$$S_2 = \begin{bmatrix} 0 \\ M \\ N \end{bmatrix} \in R^{30\times12}, \quad (4)$$

where

$$M = \begin{bmatrix} I_{3\times3} & 0 & 0 & 0 \\ 0 & 0 & 0 & 0 \\ 0 & I_{3\times3} & 0 & 0 \\ 0 & 0 & 0 & 0 \end{bmatrix} \in R^{12\times12},$$

$$N = \begin{bmatrix} 0 & I_{6\times6} \end{bmatrix} \in R^{6\times12}$$

such that $\bar{X} = XS_2 = [\omega_{RA} \ \omega_{LA} \ X_W]$. This helped in distinguishing Early_PD from the healthy control group, because PD tends to affect the unilateral side, especially with respect to arm movements, at the early stage. Therefore, the asymmetry of arm swings can be regarded as an important characteristic of Early_PD. Furthermore, Early_PD also tends to have a greater number of unstable trunk motions than is observed in healthy subjects. Therefore, the waist IMU data can also be applied to recognize deterioration due to PD onset.

Using the selected IMU data $\bar{X}$, the models were then applied using three convolutional layers with the maximum pooling sizes of 2, a flatten layer, and three fully connected layers to generate an output layer. Each convolutional layer has several filters containing a window and a max-pooling, as illustrated in Figure 5 and Table 3. The model parameters number more than sixty thousand and cannot be illustrated here. The flatten layer was then used to link the convolutional layers and the fully connected layers. Each fully connected layer contained 70 neurons.

We used ReLU [44] as the activation function for the convolutional layers and the fully connected layers. We then applied the sigmoid function [45] as the activation function of the output layer to generate two neurons. The output of

sub-model I is $Y_1 = [1 \ 0]$ or $Y_1 = [0 \ 1]$, which indicates whether the input IMU data are Adv_PD or not Adv_PD, respectively. If the input data are classified as not Adv_PD, then sub-model II is applied to estimate whether the input belongs to Early_PD or Non-PD, denoted as $Y_2 = [1 \ 0]$ or $Y_2 = [0 \ 1]$, respectively. Note that sub-model I and sub-model II have the same architecture but different model parameters because they were trained individually. During the training process, we set the batch size at 300 and the epoch at 40. We chose Adam as the optimizer and applied Dropout with a dropout rate of 10% to each hidden layer.

TABLE 3. Model dimensions.

Description	Dimensions
Input	$\bar{X} \in R^{100\times12}$
1D Convolution (5 filters, kernel size=3)	$C_1 \in R^{49\times5}$
1D Convolution (8 filters, kernel size=20)	$C_2 \in R^{15\times8}$
1D Convolution (64 filters, kernel size=5)	$C_3 \in R^{5\times64}$
Flatten	$F \in R^{320\times1}$
Fully-Connected (70 neurons)	$F_1 \in R^{70\times1}$
Fully-Connected (70 neurons)	$F_2 \in R^{70\times1}$
Fully-Connected (70 neurons)	$F_3 \in R^{70\times1}$
Output	$Y \in R^{2\times1}$

IV. RESULTS AND DISCUSSION

This section introduces the model development procedures, including model training, validation, and testing, as shown in Figure 6. We collected 6540 gait cycles from the 48 subjects in Table 1, and we applied the k-fold cross-validation method with k = 5 (i.e., we divided the normalized data set fivefold for model training and validation). Each time, we used four parts to train the model and the remaining part to validate the model. Ultimately, we built five models (A, B, C, D, and E), where each model consisted of the two sub-models: sub-model I and sub-model II. We then recruited new patients with PD and new healthy elderly subjects to test the five models.
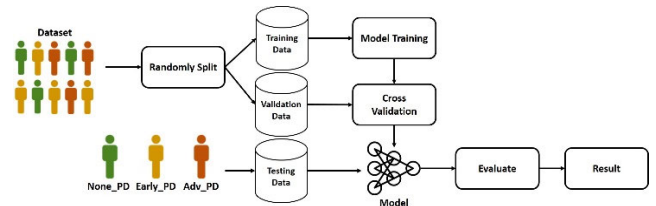

FIGURE 6. Training and validation of the neural network models.

The performance of a neural network model is usually represented as a confusion matrix [46], as illustrated in Table 4. Based on the confusion matrix, the model performance can be evaluated by the following indexes:

$$Accuracy = \frac{TP+TN}{TP+FP+FN+TN}, \quad (5)$$

TABLE 4. The confusion matrix.

Model Prediction		Ground truth	
		Positive	Negative
	Positive	TP	FP
	Negative	FN	TN

$$Precision = \frac{TP}{TP+FP}, \qquad (6)$$

$$Sensitivity = \frac{TP}{TP+FN}, \qquad (7)$$

$$Specificity = \frac{TN}{TN+FP}, \qquad (8)$$

$$F1 - score = \frac{2 \cdot TP}{2 \cdot TP+FP+FN}. \qquad (9)$$

We combined the two sub-models to classify the input data as Adv_PD, Early_PD, or Non-PD. The confusion matrix can be represented as Table 5. The performance of sub-model I in identifying Adv_PD is defined as follows:

$$Accuracy_1$$
$$= \frac{M_{11}+M_{22}+M_{23}+M_{32}+M_{33}}{M_{11}+M_{12}+M_{13}+M_{21}+M_{22}+M_{23}+M_{31}+M_{32}+M_{33}} \qquad (10)$$

$$Precision_1$$
$$= \frac{M_{11}}{M_{11} + M_{12} + M_{13}}, \qquad (11)$$

$$Sensitivity_1$$
$$= \frac{M_{11}}{M_{11} + M_{21} + M_{31}}, \qquad (12)$$

$$Specificity_1$$
$$= \frac{M_{22} + M_{23} + M_{32} + M_{33}}{M_{12} + M_{13} + M_{22} + M_{23} + M_{32} + M_{33}}, \qquad (13)$$

$$F1 - score_1$$
$$= \frac{2 \cdot M_{11}}{2 \cdot M_{11} + M_{12} + M_{13} + M_{21} + M_{31}}. \qquad (14)$$

Similarly, the performance of sub-model II in recognizing Early_PD is quantified as follows:

$$Accuracy_2 = \frac{M_{22} + M_{33}}{M_{22} + M_{23} + M_{32} + M_{33}}, \qquad (15)$$

$$Precision_2 = \frac{M_{22}}{M_{22} + M_{23}}, \qquad (16)$$

$$Sensitivity_2 = \frac{M_{22}}{M_{22} + M_{32}}, \qquad (17)$$

$$Specificity_2 = \frac{M_{33}}{M_{23} + M_{33}}, \qquad (18)$$

$$F1 - score_2 = \frac{2 \cdot M_{22}}{2 \cdot M_{22} + M_{23} + M_{32}}. \qquad (19)$$

The confusion matrixes in the model validation processes are illustrated in Table 6, where the five models achieved an average $Accuracy_1$ of 92.72%, an average $Precision_1$

of 79.86%, an average $Sensitivity_1$ of 99.51%, an average $Specificity_1$ of 90.02%, and an average $F1-score_1$ of 88.60% for identifying Adv_PD. For differentiating Early_PD and Non-PD, the five models achieved an average $Accuracy_2$ of 99.67%, an average $Precision_2$ of 99.71%, an average $Sensitivity_2$ of 99.24%, an average $Specificity_2$ of 99.86%, and an average $F1 - score_2$ of 99.48% in the validation processes.

TABLE 5. Confusion matrix for the three-class classification models.

Model Prediction		Ground Truth		
		Adv_PD	Early_PD	Non-PD
	Adv_PD	M_{11}	M_{12}	M_{13}
	Early_PD	M_{21}	M_{22}	M_{23}
	Non-PD	M_{31}	M_{32}	M_{33}

TABLE 6. Confusion matrix for model validation.

Model	Prediction	Ground Truth		
		Adv_PD	Early_PD	Non-PD
A	Adv_PD	365	71	60
	Early_PD	0	247	4
	Non-PD	0	2	559
B	Adv_PD	363	28	49
	Early_PD	2	289	3
	Non-PD	1	2	571
C	Adv_PD	389	46	63
	Early_PD	0	245	1
	Non-PD	1	4	559
D	Adv_PD	358	55	36
	Early_PD	1	269	0
	Non-PD	0	2	587
E	Adv_PD	368	47	48
	Early_PD	0	267	0
	Non-PD	2	1	575

Finally, we recruited another independent set of 36 drug-naïve patients with PD and 18 healthy elderly controls to test the developed neural network models. The patients' stages and affected sides were labelled by doctors with more than 15 years of daily experience with PD patients. These subjects' data are shown in Appendix D, and their IMU data are illustrated in Appendix B. Note that these gait data were not applied in either the training or the validation processes. We partitioned their IMU data according to the right MS and the left MS. For the subjects with PD, only the data on the affected sides were used for sub-model I to identify Adv_PD. For example, TS1 was a patient at the advanced stage, with the right side as the affected side. Therefore, we applied the IMU data from the right foot and the right arm $\begin{bmatrix} X_{RF} & X_{RA} \end{bmatrix}$ to sub-model I. For the healthy subjects (TS37–TS54), we used the IMU data on both sides for sub-model I. We then applied the angular velocities from the arms and the IMU data on the waist $\begin{bmatrix} \omega_{RA} & \omega_{LA} & X_W \end{bmatrix}$ to sub-model II to differentiate Early_PD from Non-PD.

We applied the five models (A, B, C, D, and E) to classify PD and the PD stages of these 54 subjects. The identification results of all models are illustrated in Appendix E. The model classified a subject as Adv_PD if more than 50% of the subject's gaits were identified as Adv_PD. Otherwise, the subject was labeled as not Adv_PD, and sub-models II were applied to distinguish the subject as Early_PD and Non-PD. Similarly, a subject was categorized as Early_PD if more than 50% of the gaits that were not Adv_PD gaits were identified as Early_PD. Otherwise, the subject was labeled as Non-PD.

Because each model provides independent verdicts on all subjects, different models might give conflicting predictions. For example, TS20 is a patient at the early stage. One of the 5 sub-models I classified TS20 as Adv_PD, and then 1 of the 5 sub-models II estimated TS20 as Non-PD. That is, the developed models were trained to classify PD by recognizing the important characteristics through the complex layer structures, but they might learn incorrect features, especially when the training data are limited. Therefore, we proposed a voting mechanism, where the final decision was made by the verdicts of a majority of the models. For instance, TS20 was estimated as Early_PD, because 4 sub-models I estimated the subject as not Adv_PD and 4 sub-models II estimated the subject as Early_PD. Similarly, TS41 and TS44 were both classified as Non-PD because 3 sub-models I estimated the subjects as not Adv_PD and 5 sub-models II judged the subject as Non-PD. The prediction results based on this voting mechanism are illustrated in Table 7.

First, all patients at the advanced stage were successfully classified as Adv_PD. Second, fifteen of the eighteen patients at the early stage were correctly classified as Early_PD, while three of them were estimated as Non-PD. Third, seventeen of the eighteen healthy controls were recognized as Non-PD, while one (TS46) was estimated as Adv_PD. Ultimately, the developed neural network models and voting mechanism achieved an $Accuracy_1$ of 98.15%, a $Precision_1$ of 94.74%, a $Sensitivity_1$ of 100%, a $Specificity_1$ of 97.22%, and an $F1-score_1$ of 97.30% for identifying Adv_PD in the testing processes.. Second, for classifying Early_PD and Non-PD, the neural network models and voting mechanism achieved an $Accuracy_2$ of 91.43%, a $Precision_2$ of 100%, a $Sensitivity_2$ of 83.33%, a $Specificity_2$ of 100%, and an $F1-score_2$ of 90.91% in the testing processes.

TABLE 7. Model predictions for the testing subjects.

	Ground Truth		
Prediction	Adv_PD	Early_PD	Non-PD
Adv_PD	18	0	1
Early_PD	0	15	0
Non-PD	0	3	17

V. CONCLUSION

This paper investigated the identification of PD patients. We developed neural network models for distinguishing

(a) IMU data from the right foot

(b) IMU data from the left foot

(c) IMU data from the right arm

(d) IMU data from the left arm
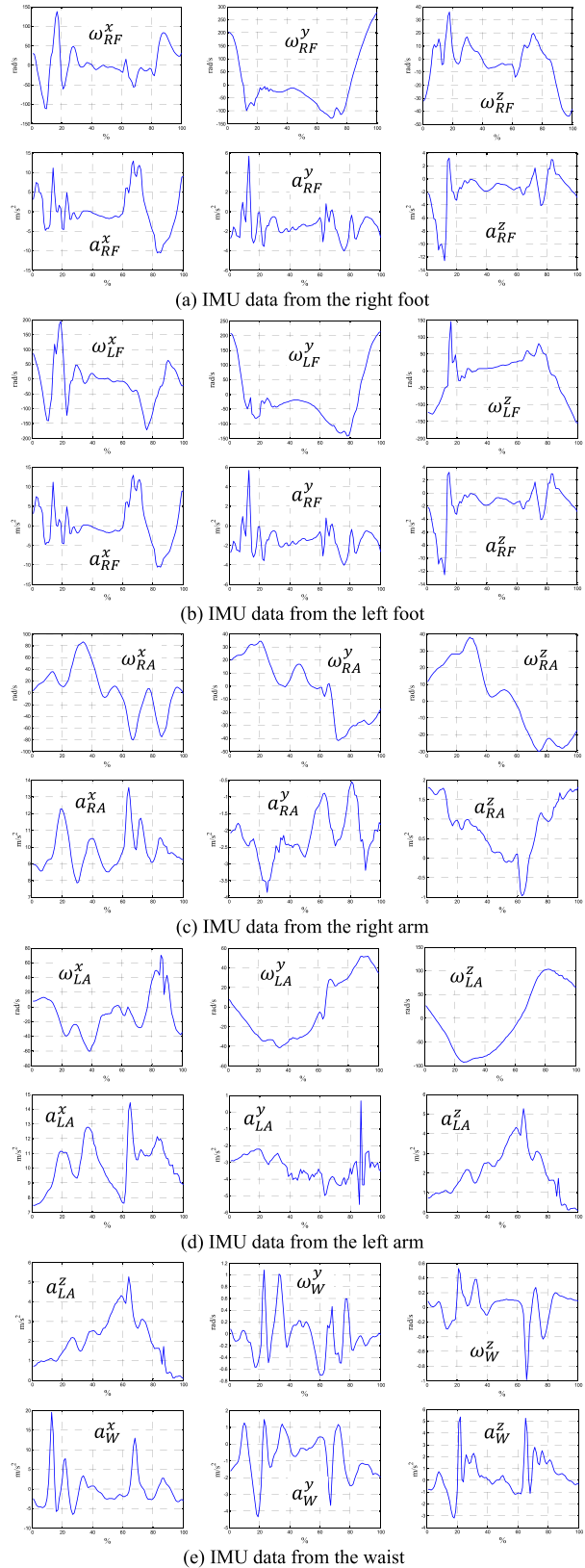
(e) IMU data from the waist

FIGURE 7. The IMU data of PD22.

patients with PD from the normal elderly population and, furthermore, for differentiating patients with early-stage

PD from those with advanced-stage PD. Early detection of PD enables the timely initiation of therapeutic management to reduce disease progression and decrease patient morbidity. Early differentiation of a PD gait from a senile gait that might be common in the normal elderly population is sometimes challenging; therefore, establishing an objective model for classifying gait characteristics is important when treating patients with PD, as well as patients with different levels of disease severity.

In this paper, we used clinical data measurements to develop neural network models that can detect and classify PD based on a subject's motion data obtained from IMUs. Because the symptoms of PD might vary significantly as the disease progresses, the proposed models consisted of two sub-models. The first sub-model estimated whether the data were compatible with Adv_PD, while the second sub-model distinguished Early_PD from the healthy control group. We applied the k-fold validation method for model training and validation, and the model achieved an accuracy of 92.72% in detecting Adv_PD and an accuracy of 99.67% in distinguishing Early_PD in model validation. Finally, we recruited new subjects to test the developed models.

Because the trained models made independent judgments and might provide conflicting results, we also introduced a voting mechanism that provided final verdicts based on the estimations of the majority of the models. The results confirmed the effectiveness of the neural network models and the voting mechanism in successfully distinguishing the Adv_PD, Early_PD, and control groups. These results indicate that the developed neural network models could help physicians to diagnose PD at an early stage, thereby allowing timely treatment in the golden time window offered during the transition from a senile gait to a diseased gait pattern. The models and voting mechanism could also be applied to differentiate Early_PD from Adv_PD as a surrogate monitoring gait marker for disease progression in PD. A future large-scale study enrolling more patients with PD is needed to validate the effectiveness of our established structure.

We could also apply the IMU data from the testing subjects to develop new neural network models and add them to the voting mechanism to improve the accuracy of PD predictions. In the future, we plan to extend these PD gait models to distinguish patients with PD from those with atypical parkinsonism that can initially present with PD-like symptoms but has a worse future prognosis. The developed model structures might also be applied to the classification of other diseases, such as the discrimination between benign tremors and early PD, if enough samples are available.

.

APPENDIX A

The studies were approved by the Human Subject Research Ethics Committee of the Institutional Review Board (IRB), available at: http://140.112.14.7/~sic/PaperMaterial/IRB_PD.pdf

TABLE 8. Basic data of the testing subjects.

Subjects	Gender	Age	PD Stage	Side
TS1	F	77	Adv-PD	R
TS2	F	68	Adv-PD	R
TS3	F	86	Adv-PD	R
TS4	M	88	Adv-PD	R
TS5	M	75	Adv-PD	R
TS6	M	84	Adv-PD	L
TS7	M	79	Adv-PD	L
TS8	F	67	Adv-PD	L
TS9	M	71	Adv-PD	L
TS10	M	73	Adv-PD	L
TS11	M	72	Adv-PD	R
TS12	F	83	Adv-PD	L
TS13	F	76	Adv-PD	R
TS14	M	81	Adv-PD	L
TS15	M	79	Adv-PD	R
TS16	M	50	Adv-PD	L
TS17	F	70	Adv-PD	R
TS18	F	71	Adv-PD	L
TS19	F	76	Early-PD	R
TS20	M	87	Early-PD	R
TS21	F	59	Early-PD	R
TS22	F	56	Early-PD	R
TS23	F	54	Early-PD	L
TS24	F	78	Early-PD	L
TS25	F	79	Early-PD	L
TS26	F	67	Early-PD	L
TS27	F	66	Early-PD	L
TS28	M	76	Early-PD	L
TS29	F	69	Early-PD	R
TS30	M	51	Early-PD	R
TS31	M	50	Early-PD	R
TS32	M	71	Early-PD	R
TS33	M	78	Early-PD	R
TS34	F	77	Early-PD	L
TS35	F	66	Early-PD	R
TS36	M	70	Early-PD	L
TS37	M	69	Non-PD	
TS38	M	72	Non-PD	
TS39	F	72	Non-PD	
TS40	F	65	Non-PD	
TS41	F	71	Non-PD	
TS42	F	73	Non-PD	
TS43	M	77	Non-PD	
TS44	F	72	Non-PD	
TS45	F	69	Non-PD	
TS46	F	76	Non-PD	
TS47	F	74	Non-PD	
TS48	M	74	Non-PD	
TS49	F	77	Non-PD	
TS50	F	73	Non-PD	
TS51	F	67	Non-PD	
TS52	F	69	Non-PD	
TS53	M	71	Non-PD	
TS54	M	74	Non-PD	

APPENDIX B
The IMU data of all participants are available at: http://140.112.14.7/∼sic/PaperMaterial/PD_Appendix_B_IMU_data.zip

APPENDIX C
The IMU data of PD22. See Figure 7.

APPENDIX D
Basic data of the testing subjects. See Table 8.

APPENDIX E
http://140.112.14.7/∼sic/PaperMaterial/PD_Appendix_E.pdf

REFERENCES

[1] E. R. Dorsey, R. Constantinescu, J. P. Thompson, K. M. Biglan, R. G. Holloway, K. Kieburtz, F. J. Marshall, B. M. Ravina, G. Schifitto, A. Siderowf, and C. M. Tanner, "Projected number of people with Parkinson disease in the most populous nations, 2005 through 2030," *Neurology*, vol. 68, no. 5, pp. 384–386, 2007, doi: 10.1212/01.wnl.0000247740.47667.03.

[2] F. B. Horak, D. Dimitrova, and J. G. Nutt, "Direction-specific postural instability in subjects with Parkinson's disease," *Exp. Neurol.*, vol. 193, no. 2, pp. 504–521, Jun. 2005, doi: 10.1016/j.expneurol.2004.12.008.

[3] B. S. Connolly and A. E. Lang, "Pharmacological treatment of parkinson disease: A review," *J. Amer. Med. Assoc.*, vol. 311, no. 16, pp. 1670–1683, Apr. 2014, doi: 10.1001/jama.2014.3654.

[4] M. M. Hoehn and M. D. Yahr, "Parkinsonism: Onset, progression, and mortality," *Neurology*, vol. 50, no. 2, p. 318, Feb. 1998, doi: 10.1212/WNL.50.2.318.

[5] A. Mirelman *et al.*, "Arm swing as a potential new prodromal marker of Parkinson's disease," *Movement Disorders, Clin. Pract.*, vol. 31, no. 10, pp. 1527–1534, Oct. 2016, doi: 10.1002/mds.26720.

[6] M. Pistacchi, M. Gioulis, F. Sanson, E. D. Giovannini, G. Filippi, F. Rossetto, and S. Z. Marsala, "Gait analysis and clinical correlations in early Parkinson's disease," *Funct. Neurol.*, vol. 32, no. 1, p. 28, Jan. 2017, doi: 10.11138/FNeur/2017.32.1.028.

[7] Y.-R. Yang, Y.-Y. Lee, S.-J. Cheng, P.-Y. Lin, and R.-Y. Wang, "Relationships between gait and dynamic balance in early Parkinson's disease," *Gait Posture*, vol. 27, no. 4, pp. 611–615, May 2008, doi: 10.1016/j.gaitpost.2007.08.003.

[8] N. Giladi, M. P. McDermott, S. Fahn, S. Przedborski, J. Jankovic, M. Stern, and C. Tanner, "Freezing of gait in PD: Prospective assessment in the DATATOP cohort," *Neurology*, vol. 56, no. 12, pp. 1712–1721, Jun. 2001, doi: 10.1212/WNL.56.12.1712.

[9] K. Jahn, A. Zwergal, and R. Schniepp, "Gait disturbances in old age: Classification, diagnosis, and treatment from a neurological perspective," *Deutsches Ärzteblatt Int.*, vol. 107, no. 17, p. 306, Apr. 2010, doi: 10.3238/arztebl.2010.0306.

[10] A. Saad, I. Zaarour, A. Zeinedine, M. Ayache, P. Bejjani, F. Guerin, D. Lefebvre, and L. Havre-France, "A preliminary study of the causality of freezing of gait for Parkinson's disease patients: Bayesian belief network approach," *Int. J. Comput. Sci. Issues*, vol. 10, no. 3, pp. 88–95, Dec. 2013. [Online]. Available: https://www.ijcsi.org/papers/IJCSI-10-3-2-88-95.pdf

[11] E. E. Tripoliti, A. T. Tzallas, M. G. Tsipouras, G. Rigas, P. Bougia, M. Leontiou, S. Konitsiotis, M. Chondrogiorgi, S. Tsouli, and D. I. Fotiadis, "Automatic detection of freezing of gait events in patients with Parkinson's disease," *Comput. Methods Programs Biomed.*, vol. 110, no. 1, pp. 12–26, Apr. 2013, doi: 10.1016/j.cmpb.2012.10.016.

[12] A. P. Rocha, H. Choupina, J. M. Fernandes, M. J. Rosas, R. Vaz, and J. P. S. Cunha, "Parkinson's disease assessment based on gait analysis using an innovative RGB-D camera system," in *Proc. 36th Annu. Int. Conf. IEEE Eng. Med. Biol. Soc.*, Aug. 2014, pp. 3126–3129, doi: 10.1109/EMBC.2014.6944285.

[13] M. R. Daliri, "Chi-square distance kernel of the gaits for the diagnosis of Parkinson's disease," *Biomed. Signal Process. Control*, vol. 8, no. 1, pp. 66–70, Jan. 2013, doi: 10.1016/j.bspc.2012.04.007.

[14] F. Wahid, R. K. Begg, C. J. Hass, S. Halgamuge, and D. C. Ackland, "Classification of Parkinson's disease gait using spatial-temporal gait features," *IEEE J. Biomed. Health Inform.*, vol. 19, no. 6, pp. 1794–1802, Nov. 2015, doi: 10.1109/JBHI.2015.2450232.

[15] A. Caliskan, H. Badem, A. Basturk, and M. E. Yuksel, "Diagnosis of the Parkinson disease by using deep neural network classifier," *Istanbul Univ., J. Elect. Electron. Eng.*, vol. 17, no. 2, pp. 3311–3318, 2017. [Online]. Available: https://electricajournal.org/Content/files/sayilar/58/3311-3318.pdf

[16] M. S. Baby, A. J. Saji, and C. S. Kumar, "Parkinsons disease classification using wavelet transform based feature extraction of gait data," in *Proc. Int. Conf. Circuit, Power Comput. Technol. (ICCPCT)*, Apr. 2017, pp. 1–6, doi: 10.1109/ICCPCT.2017.8074230.

[17] A. Samà, C. Pérez-López, D. Rodríguez-Martín, A. Català, J. M. Moreno-Aróstegui, J. Cabestany, E. de Mingo, and A. Rodríguez-Molinero, "Estimating bradykinesia severity in Parkinson's disease by analysing gait through a waist-worn sensor," *Comput. Biol. Med.*, vol. 84, pp. 114–123, May 2017, doi: 10.1016/j.compbiomed.2017.03.020.

[18] H. B. Kim, W. W. Lee, A. Kim, H. J. Lee, H. Y. Park, H. S. Jeon, S. K. Kim, B. Jeon, and K. S. Park, "Wrist sensor-based tremor severity quantification in Parkinson's disease using convolutional neural network," *Comput. Biol. Med.*, vol. 95, pp. 140–146, Apr. 2018, doi: 10.1016/j.compbiomed.2018.02.007.

[19] A. Ul Haq, J. Li, M. H. Memon, J. Khan, S. U. Din, I. Ahad, R. Sun, and Z. Lai, "Comparative analysis of the classification performance of machine learning classifiers and deep neural network classifier for prediction of Parkinson disease," in *Proc. 15th Int. Comput. Conf. Wavelet Act. Media Technol. Inf. Process. (ICCWAMTIP)*, Dec. 2018, pp. 101–106, doi: 10.1109/ICCWAMTIP.2018.8632613.

[20] S. Bilgin and Z. E. Akin, "Gait pattern discrimination of ALS patients using classification methods," *Turkish J. Electr. Eng. Comput. Sci.*, vol. 26, no. 3, pp. 1367–1377, 2018, doi: 10.3906/elk-1708-221.

[21] E. Abdulhay, N. Arunkumar, K. Narasimhan, E. Vellaiappan, and V. Venkatraman, "Gait and tremor investigation using machine learning techniques for the diagnosis of Parkinson disease," *Future Gener. Comput. Syst.*, vol. 83, pp. 366–373, Jun. 2018, doi: 10.1016/j.future.2018.02.009.

[22] E. Rastegari, S. Azizian, and H. Ali, "Machine learning and similarity network approaches to support automatic classification of Parkinson's diseases using accelerometer-based gait analysis," in *Proc. 52nd Hawaii Int. Conf. Syst. Sci. (HICSS)*, Jan. 2019, pp. 4231–4242, doi: 10.24251/HICSS.2019.511.

[23] N. S. Hoang, Y. Cai, C.-W. Lee, Y. O. Yang, C.-K. Chui, and M. C. Heng Chua, "Gait classification for Parkinson's disease using stacked 2D and 1D convolutional neural network," in *Proc. Int. Conf. Adv. Technol. Commun. (ATC)*, Oct. 2019, pp. 44–49, doi: 10.1109/ATC.2019.8924567.

[24] K. Hu, Z. Wang, S. Mei, K. A. E. Martens, T. Yao, S. J. G. Lewis, and D. D. Feng, "Vision-based freezing of gait detection with anatomic directed graph representation," *IEEE J. Biomed. Health Informat.*, vol. 24, no. 4, pp. 1215–1225, Apr. 2020, doi: 10.1109/JBHI.2019.2923209.

[25] G. Solana-Lavalle, J.-C. Galán-Hernández, and R. Rosas-Romero, "Automatic Parkinson disease detection at early stages as a pre-diagnosis tool by using classifiers and a small set of vocal features," *Biocybern. Biomed. Eng.*, vol. 40, no. 1, pp. 505–516, Jan. 2020, doi: 10.1016/j.bbe.2020.01.003.

[26] S. Sivaranjini and C. M. Sujatha, "Deep learning based diagnosis of Parkinson's disease using convolutional neural network," *Multimedia Tools Appl.*, vol. 79, nos. 21–22, pp. 15467–15479, Jun. 2020, doi: 10.1007/s11042-019-7469-8.

[27] F. Aydın and Z. Aslan, "Recognizing Parkinson's disease gait patterns by vibes algorithm and Hilbert–Huang transform," *Eng. Sci. Technol., Int. J.*, vol. 24, no. 1, pp. 112–125, Feb. 2021, doi: 10.1016/j.jestch.2020.12.005.

[28] I. El Maachi, G.-A. Bilodeau, and W. Bouachir, "Deep 1D-convnet for accurate Parkinson disease detection and severity prediction from gait," *Expert Syst. Appl.*, vol. 143, Apr. 2020, Art. no. 113075, doi: 10.1016/j.eswa.2019.113075.

[29] B. Karan and S. Sekhar Sahu, "An improved framework for Parkinson's disease prediction using variational mode decomposition-Hilbert spectrum of speech signal," *Biocybern. Biomed. Eng.*, vol. 41, no. 2, pp. 717–732, Apr. 2021, doi: 10.1016/j.bbe.2021.04.014.

[30] H. Gunduz, "An efficient dimensionality reduction method using filter-based feature selection and variational autoencoders on Parkinson's disease classification," *Biomed. Signal Process. Control*, vol. 66, Apr. 2021, Art. no. 102452, doi: 10.1016/j.bspc.2021.102452.

[31] D. Yang, K.-S. Hong, S.-H. Yoo, and C.-S. Kim, "Evaluation of neural degeneration biomarkers in the prefrontal cortex for early identification of patients with mild cognitive impairment: An fNIRS study," *Frontiers Hum. Neurosci.*, vol. 13, p. 317, Sep. 2019, doi: 10.3389/fnhum.2019.00317.

[32] D. Yang, R. Huang, S.-H. Yoo, M.-J. Shin, J. A. Yoon, Y.-I. Shin, and K.-S. Hong, "Detection of mild cognitive impairment using convolutional neural network: Temporal-feature maps of functional near-infrared spectroscopy," *Frontiers Aging Neurosci.*, vol. 12, p. 141, May 2020, doi: 10.3389/fnagi.2020.00141.

[33] S.-H. Yoo, S.-W. Woo, M.-J. Shin, J. A. Yoon, Y.-I. Shin, and K.-S. Hong, "Diagnosis of mild cognitive impairment using cognitive tasks: A functional near-infrared spectroscopy study," *Current Alzheimer Res.*, vol. 17, no. 13, pp. 1145–1160, Mar. 2021, doi: 10.2174/1567205018666210212154941.

[34] D. Yang and K.-S. Hong, "Quantitative assessment of resting-state for mild cognitive impairment detection: A functional near-infrared spectroscopy and deep learning approach," *J. Alzheimer's Disease*, vol. 80, no. 2, pp. 647–663, Mar. 2021, doi: 10.3233/jad-201163.

[35] L. C. Guayacán and F. Martínez, "Visualising and quantifying relevant parkinsonian gait patterns using 3D convolutional network," *J. Biomed. Informat.*, vol. 123, Nov. 2021, Art. no. 103935, doi: 10.1016/j.jbi.2021.103935.

[36] A. J. Hughes, S. E. Daniel, L. Kilford, and A. J. Lees, "Accuracy of clinical diagnosis of idiopathic Parkinson's disease: A clinico-pathological study of 100 cases," *J. Neurol., Neurosurg., Psychiatry*, vol. 55, pp. 181–184, Mar. 1992, doi: 10.1136/jnnp.55.3.181.

[37] D. Mungas, "In-office mental status testing: A practical guide," *Geriatrics*, vol. 46, no. 7, pp. 54–67, Jul. 1991.

[38] APDM. *Opal User Guide*. Accessed: Oct. 2021. [Online]. Available: https://www.apdm.com

[39] K. Aminian, B. Najafi, C. Büla, P. F. Leyvraz, and P. Robert, "Spatio-temporal parameters of gait measured by an ambulatory system using miniature gyroscopes," *J. Biomech.*, vol. 35, no. 5, pp. 689–699, May 2002, doi: 10.1016/S0021-9290(02)00008-8.

[40] F.-C. Wang, Y.-C. Li, K.-L. Wu, P.-Y. Chen, and L.-C. Fu, "Online gait detection with an automatic mobile trainer inspired by neuro-developmental treatment," *Sensors*, vol. 20, no. 12, p. 3389, Jun. 2020, doi: 10.3390/s20123389.

[41] S. Bind, A. K. Tiwari, A. K. Sahani, P. Koulibaly, F. Nobili, M. Pagani, O. Sabri, T. V. Borght, K. V. Laere, and K. Tatsch, "A survey of machine learning based approaches for Parkinson disease prediction," *Int. J. Comput. Sci. Inf. Technol.*, vol. 6, no. 2, pp. 1648–1655, 2015. [Online]. Available: https://citeseerx.ist.psu.edu/viewdoc/download?doi=10.1.1.735.5660&rep=rep1&type=pdf

[42] S. B. Kotsiantis, I. Zaharakis, and P. Pintelas, "Supervised machine learning: A review of classification techniques," *Emerg. Artif. Intell. Appl. Comput. Eng.*, vol. 160, pp. 3–24, Oct. 2007. [Online]. Available: https://datajobs.com/data-science-repo/Supervised-Learning-[SB-Kotsiantis].pdf

[43] Y. LeCun, Y. Bengio, and G. Hinton, "Deep learning," *Nature*, vol. 521, no. 7553, pp. 436–444, May 2015, doi: 10.1038/nature14539.

[44] S. Sharma, S. Sharma, and A. Athaiya, "Activation functions in neural networks," *Towards Data Sci.*, vol. 6, no. 12, pp. 310–316, 2017. [Online]. Available: https://www.ijeast.com/papers/310-316,Tesma412,IJEAST.pdf

[45] B. Karlik and A. Vehbi, "Performance analysis of various activation functions in generalized MLP architectures of neural networks," *Int. J. Artif. Intell. Expert Syst.*, vol. 1, no. 4, pp. 111–122, 2011. [Online]. Available: https://citeseerx.ist.psu.edu/viewdoc/download?doi=10.1.1.740.9413&rep=rep1&type=pdf

[46] D. M. W. Powers, "Evaluation: From precision, recall and F-measure to ROC, informedness, markedness and correlation," Oct. 2020, *arXiv:2010.16061*.

CHIN-HSIEN LIN received the Graduate degree from the College of Medicine, National Taiwan University, the neurological residency training from National Taiwan University Hospital (NTUH), and the Ph.D. degree from the Institute of Molecular Biology, Academia Sinica. In Ph.D. degree, she investigated the molecular mechanisms of LRRK2 mutations in neurons by using a Drosophila model system. She received the Postdoctoral Fellowship training with the Center for Applied Neurogenetics, The University of British Columbia, Canada.

She is currently a Clinical Professor with the Department of Neurology, National Taiwan University Hospital. Her research interests include genetic and molecular biology studies of Parkinson's disease and related neurodegenerative disorders. She investigated the molecular mechanisms of mutations of Parkinson's disease causative genes in neuronal degeneration by using cellular and animal model systems. She is also investigating the gut-brain axis mechanism in the pathogenesis of neurodegeneration. She is also an Executive Member of Taiwan Movement Disorders Society, a Representative Member of the Leadership Program of International Movement Disorder Society. She is also a Committee Member of Educational Committee of the MDS-AOS Section, and an Active Member of Evidence-Based Medicine (EMB) and Basic Neuroscience Committees of International Movement Disorders Society.

FU-CHENG WANG (Senior Member, IEEE) received the B.S. and M.Sc. degrees from the Mechanical Engineering Department, National Taiwan University, and the Ph.D. degree in control engineering from the Engineering Department, Cambridge University, U.K.

He joined the Department of Mechanical Engineering, National Taiwan University, in 2003. His research interests include robust control, vibration control, system integration, medical engineering, and energy systems. He served as an Associate Editor for *ASME Journal of Dynamic Systems, Measurement and Control*, from 2013 to 2016. He has been served as an Associate Editor for the *Proceedings of the Institution of Mechanical Engineers Part—I: Journal of Systems and Control Engineering*, since 2020, and the Editorial Board Member for *Machines*, since 2021.

TIEN-YUN KUO received the B.S. degree from the Department of Mechanical Engineering, National Chung Cheng University, in 2018. He is currently pursuing the M.S. degree with the Mechanical Engineering Department, National Taiwan University. His current research interests include robust control, system integration, biomedical engineering, and machine learning.

PO-WEI HUANG received the B.S. degree from the Department of Mechanical Engineering, National Taiwan University, in 2021, where he is currently pursuing the M.S. degree with the Mechanical Engineering Department. His current research interests include robust control, system integration, biomedical engineering, and machine learning.

SZU-FU CHEN received the M.D. degree from Kaohsiung Medical University, Taiwan, and the Ph.D. degree in neuroscience from the Brain Repair Center, Cambridge University, U.K. She is currently the Director of the Neurological Division, Department of Physical Medicine Rehabilitation, Cheng Hsin General Hospital, and a Professor with the Department of Physiology, National Defense Medical Center, Taiwan. Her research interests include pathobiology and treatment of traumatic brain injury and stroke, mechanisms of cell death, and neuroinflammation, while her clinical interests consist of rehabilitation of brain damage and spinal cord injury, and peripheral nerve injuries.

LI-CHEN FU (Fellow, IEEE) received the B.S. degree from the National Taiwan University, Taiwan, in 1981, and the M.S. and Ph.D. degrees from the University of California at Berkeley, Berkeley, USA, in 1985 and 1987, respectively.

Since 1987, he has been joined the National Taiwan University, and has been awarded Irving T. Ho Chair Professor and NTU Chair Professor, since 2007 and 2020, respectively. He is currently working as the Director of the NTU Center for Artificial Intelligence (AI) and Advanced Robotics, and the Co-Director of the Ministry of Science and Technology (MOST)/NTU Joint Research Center for AI Technology and All Vista Healthcare. So far, he has received numerous academic recognitions, such as Distinguished Research Awards from National Science Council, Taiwan, Macronix Chair Professorship, Academic Award, and National Chair Professorship from the Ministry of Education, Taiwan, and IFAC Fellow, in 2017. He is also serving as the Editor-in-Chief of the *Asian Journal of Control* and an Advisory Committee Member of Asian Control Association. He has served as the Vice-President of IEEE Control Systems Society, from 2017 to 2018. His research interests include social robotics, smart home, visual detection and tracking, virtual reality, and control theory and applications.

• • •